Plasmonic diffraction for the sensitivity enhancement of silicon image sensor

Atsushi Ono[1,2], Kazuma Hashimoto[1], Takahito Yoshinaga[1], and Nobukazu Teranishi[2,3]

1 Graduate School of Integrated Science and Technology, Shizuoka University,
3-5-1 Johoku Hamamatsu Japan
2 Research Institute of Electronics, Shizuoka University, 3-5-1 Johoku Hamamatsu Japan
3 Laboratory of Advanced Science and Technology for Industry, University of Hyogo,
1-1-2 Koto, Kamigori, Ako-gun, Hyogo Japan
e-mail: ono.atsushi@shizuoka.ac.jp **TEL:** +81-53-478-1370 **FAX:** +81-53-478-1651

Introduction

Near-infrared (NIR) sensing technology has been extensively applied in biological inspection, Time-of-Flight (ToF), surveillance, and fiber optic communication. A wavelength of 940 nm is mostly used as their light source, because it is completely invisible to the human eye and is less affected by sunlight. However, silicon-based image sensors have insufficient sensitivity in NIR region because of the low silicon absorption. Although a thick silicon absorption layer improves NIR sensitivity, this approach degrades image recognition due to the crosstalk between pixels and is technically difficult to be implemented in deep trench isolation (DTI). Therefore, improving the NIR light sensitivity without a thick silicon layer is a significant issue. In recent years, a multiple pyramid shape surface of silicon sensitive layer has been proposed and developed to increase the light propagation length and effective silicon thickness by light diffraction [1].

Applying plasmonic enhancement also has the potential to improve the NIR sensitivity of sensors. Plasmonics has been applied in the photonics research field, ranging from ultraviolet to infrared, such as fluorescence enhancement, surface enhanced Raman scattering, solar cells, color filters, and thermal emission control. In sensor applications, the development of silicon metal Schottky junction-type photodetectors using plasmon hot carriers and enhanced electric fields by surface plasmon resonance have attracted attention in the detection of photon energies below silicon bandgap of 1.12 eV [2-8]. Most of the approaches in plasmonics to photonics applications have included the utilization of strong electric field enhancement, which involves resonant coupling between photons and electrons in metal. In this study, we apply the quasi-resonant conditions of surface plasmons to improve the silicon absorption efficiency [9].

NIR sensitivity improvement by metal gratings and metal DTI

We propose a plasmonic image sensor constructed by the metal gratings of surface plasmon diffraction and highly reflective metal DTI of the reflection of the diffracted light to improve the NIR absorption of silicon (Fig. 1). An enhanced electric field was generated near the metal surface due to the surface plasmon resonance. Under rigidly resonant conditions, the photon energy couples with electronic vibration and is converted to propagate on the metal surface, so the wave vector of the coupled light is orthogonal. Conversely, by slightly shifting the diffraction condition from the orthogonal condition, the light propagates to the silicon side. The diffracted light under conditions close to 90° is reflected by the DTI formed along the pixel boundary. Repetition reflection increases the effective propagation length of the silicon. A large diffraction angle and high diffraction efficiency increase sensitivity. Moreover, because it is close to the plasmon resonance, the reflectance from the sensor surface is suppressed, and the light utilization efficiency is improved. In this study, we investigated the conditions that maximize the absorption efficiency in silicon from the viewpoint of diffraction angle and diffraction efficiency for NIR at a wavelength of 940 nm.

A silver grating was applied for the plasmonic diffraction (Fig.2(a)). The period determines the diffraction angle. The synchronization mode of surface plasmon resonance was tuned to a wavelength of 940 nm by changing the metal line width with respect to the period. The metal height mainly contributed to the diffraction efficiency. The silver diffraction grating was covered with an SiO_2
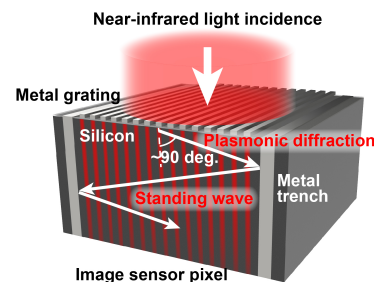

Fig. 1 Schematic diagram of the plasmonic image sensor with metal gratings and highly reflective metal DTI.
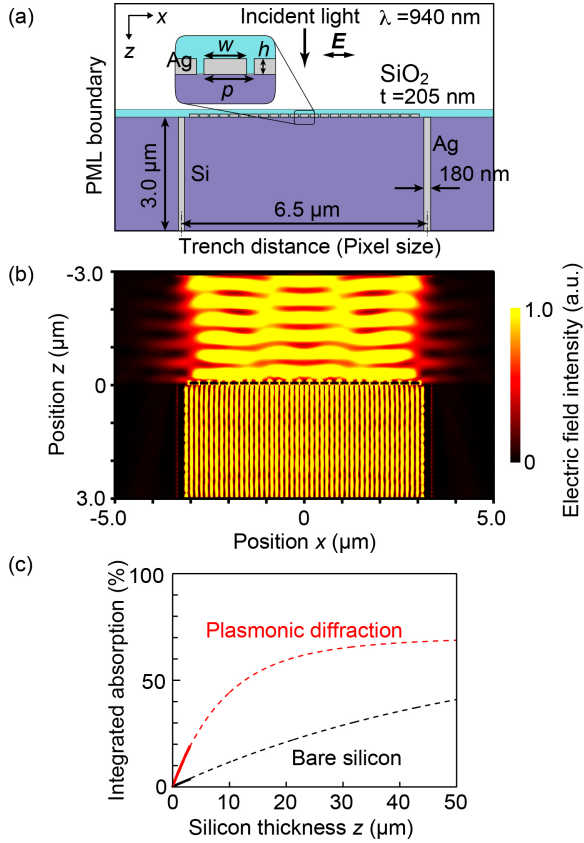
Fig. 2 Simulation results for the plasmonic silicon image sensor constructed by silver gratings combined with silver DTI. (a) Simulation model, (b) electric-field intensity distribution, (c) integrated absorptions of silicon in thickness with and without plasmonic diffraction.

layer for protection. A natural oxide film with a thickness of 2 nm was remained on the silicon surface. Silver was buried in the DTI. The pixel size was set to 6.5 μm. Transmittance represents the light intensity ratio of the 0th-order light monitored at a silicon thickness of 3 μm. Reflection represents the ratio of the reflection to the normal angle. The backward scattering and the forward scattering were monitored on sides via the silver diffraction grating, respectively. In Fig. 2, silver trench was set in forward side. Therefore, we set a trench absorption monitor instead of the forward scattering monitor. The structural parameters of the silver diffraction gratings were optimized for the maximum silicon absorption at a wavelength of 940 nm in the region from the Si surface to a depth of 3.0 μm. A finite-difference time-domain simulation and rigorous coupled wave analysis were performed using commercially available software FullWAVE and DiffractMOD by RSOFT. The optimized period, width, and height of the silver grating were 265 nm, 230 nm, and 85 nm, respectively. The covered SiO$_2$ layer thickness was 205 nm. The propagation wavelength λ_{si} of light with a wavelength of 940 nm in silicon was $\lambda_{si} = \lambda_o/n_{si} \simeq 261$ nm, which is slightly

shorter than the period. The diffraction angle for a period of 265 nm was 80.6°.

By reflecting the diffracted light in the trench, the effective propagation length in silicon increased, and the absorption efficiency was improved. When the diffraction angle was 80.6°, the effective propagation distance was six times compared with a sensor without silver grating. Figure 2(b) shows the electric field intensity distribution of the x-z cross section when the optimized silver diffraction grating is irradiated with NIR at a wavelength of 940 nm. Surface plasmon resonance was excited, and an enhanced electric field was formed near the surface of the silver diffraction grating. Interference fringes were observed inside the silicon. This standing wave indicates that the light diffracted by silver grating interfered with the light reflected from the trench. The absorption ratio in silicon for a thickness of 3.0 μm was enhanced to 19.2%, which was a 5.3-fold improvement over the 3.6% absorption rate of bare silicon. The fitting curve of the dashed line in Fig. 2(c) was analyzed based on the transmitted light ratio and silicon absorption ratio using the absorption simulation result of the solid line. When plasmon diffraction was applied, an absorption of 44% was achieved at a silicon thickness of 10 μm. In the case of plasmon diffraction, the silicon absorption for a wavelength of 940 nm saturated at approximately 70%. The estimated quantum efficiency is almost same as integrated absorption because the absorption in dead layer less than around 200 nm is a few percent.

Plasmonic diffraction under the quasi-resonant condition

To consider the absorption enhancement principle using plasmonic diffraction and DTI reflection, the electric field intensity distribution of the x-z cross section without DTI is shown in Fig. 3(a). The enhanced electric field on the metal surface by surface plasmon excitation contributed to the diffraction on the silicon side. The vertical stripe intensity field distribution was due to the interference between the 0th-order and the ±1st-order light. The diffracted light propagated at an angle of approximately 80°. This diffracted light, which is a factor for a standing wave in silicon, was reflected by the metal DTI as resulted in Fig. 2(b). The forward scattering was 49.7%, which was considered to be the diffraction component and indicated a high diffraction efficiency. Figure 3(b) shows the dependence of the reflectance spectrum on the incident angle. The reflectance dip-curve dispersion represents the surface plasmon resonance of the silver grating. The broken line indicates the 90° diffraction condition of the 1st-order diffracted light. The matching condition
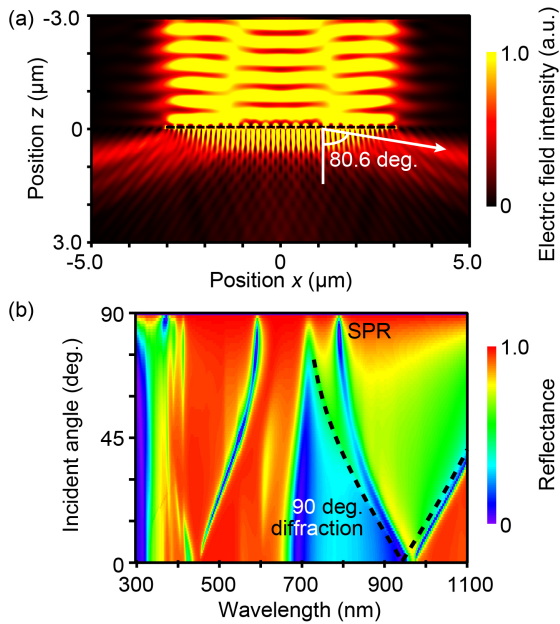
Fig. 3 (a) Electric field intensity distribution of the plasmonic diffraction by silver grating on silicon without DTI. (b) Incident angle dependence of the reflection spectra

between the surface plasmon dispersion relation and the 90° diffraction was an incident angle of 0°. The matching wavelength was 952 nm for a grating period of 265 nm. The incident wavelength of 940 nm was slightly shorter than the matching wavelength, and it diffracted at 80.6°. This quasi-resonant mechanism achieves a larger diffraction angle and diffraction efficiency than a general diffraction grating. Thus, the principle of silicon absorption enhancement with respect to NIR is that while exciting surface plasmon resonance, light is diffracted toward the silicon side with a large diffraction angle so that it efficiently propagates in the silicon in the lateral direction.

Figure 4 shows the cross-sectional enlarged view of electric field intensity distribution of silver grating on silicon. It is superimposed by vector of electric field. Surface plasmon was excited on silver, and strong enhanced electric field was observed between silver lines. From the vector flow, it was found that the quadrupole of plasmon oscillation
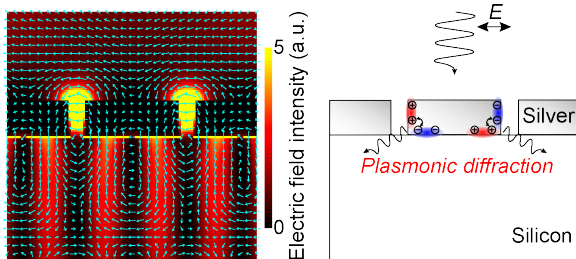
was excited. It was concluded that this quadrupole plasmon oscillation radiates photons as diffracted light with high efficiency.

DTI materials for NIR reflection

In our proposed construction, DTI in silicon pixels plays an important role in the absorption enhancement of NIR. In recent image sensors, DTI has been used as a pixel isolation method. Polycrystalline silicon, SiO_2, and tungsten (W) are mainly used inside the DTI together with the negatively charged layer. The selection of this material is important for NIR image sensors. Figure 5 shows the reflectance dependence on the incident angle at a wavelength of 940 nm for various trench materials, such as SiO_2, silver (Ag), aluminum (Al), copper (Cu), and tungsten. Each complex refractive index at a wavelength of 940 nm was 1.47 for SiO_2 [10], $0.08 + i6.78$ for Ag [11], $1.73 + i8.60$ for Al [12], $0.24 + i6.02$ for Cu [12], and $3.14 + i3.16$ for W [12]. The solid line shows the characteristics when the trench layer thickness is 50 nm, and the broken line shows for the infinite layer thickness. The most useful trench material, SiO_2, exhibited 100% reflection under conditions of sufficient thickness and total internal reflection at an incident angle of 25° or larger. However, the reflectance drastically dropped with thin DTI thickness owing to the evanescent transmission. Thus, it was unsuitable for sensor pixel miniaturization. In particular, in the case of plasmon diffraction at 80°, the trench incident angle was 10°, and its reflectance was only 20% or less even under infinite thickness conditions. Therefore, SiO_2 is not applicable for increasing the effective propagation length using a system of plasmonic diffraction and trench reflection. Metals showed relatively high reflectance in most incident angle ranges, but W, which was often used as a trench material, had low reflectance in the NIR wavelength range. Ag, Cu, and Al are recommended as trench materials for NIR image sensors. Among them, Ag had the highest reflectance, and it exhibited an angular average reflectance of 96% even at a DTI thickness of 50 nm.
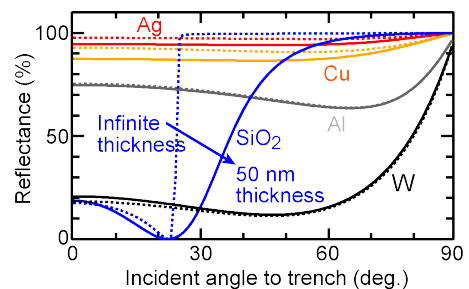

Fig. 4 Enlarged electric field intensity distribution and the vector map at the incident wavelength of 940 nm

Fig. 5 Reflectance spectra dependence on the incident angle of DTI materials of SiO_2, Ag, Cu, Al, and W at an NIR wavelength of 940 nm

Conclusions

we proposed plasmonic diffraction combined with highly reflective DTI to enhance NIR sensitivity. The metal grating period slightly detuned from the surface plasmon resonance resulted in a state with a large diffraction angle and high diffraction efficiency, which led to a significant improvement in NIR sensitivity. In addition, the detuning reduced the metal absorption loss. Silver grating with a 265 nm period, 230 nm width, and 85 nm height and silver DTI with layer thickness of 50 nm improved the sensitivity to 5.3 times at a wavelength of 940 nm for 3-μm-thick silicon image sensors compared to those without silver grating. The development of high-sensitivity NIR image sensors using plasmonic diffraction combined with highly reflective DTI could achieve small thickness sensor and small DTI thickness. Therefore, NIR CMOS image sensor with small pixel size could be realized, which might be applied to various applications, such as ToF, security, biometrics, biological inspection, and automobile.

References

[1] S. Yokogawa, I. Oshiyama, H. Ikeda, Y. Ebiko, T. Hirano, S. Saito, T. Oinoue, Y. Hagimoto, and H. Iwamoto, "IR sensitivity enhancement of CMOS Image Sensor with diffractive light trapping pixels," Sci. Rep. 7(1), 3832 (2017).

[2] M. W. Knight, H. Sobhani, P. Nordlander, and N. J. Halas, "Photodetection with Active Optical Antennas," SCIENCE 332(6030), 702–704 (2011).

[3] M. W. Knight, Y. Wang, A. S. Urban, A. Sobhani, B. Y. Zheng, P. Nordlander, and N. J. Halas, "Embedding Plasmonic Nanostructure Diodes Enhances Hot Electron Emission," Nano Lett. 13(4), 1687–1692 (2013).

[4] A. Sobhani, M. W. Knight, Y. Wang, B. Zheng, N. S. King, L. V. Brown, Z. Fang, P. Nordlander, and N. J. Halas, "Narrowband photodetection in the near-infrared with a plasmon-induced hot electron device," Nat. Commun. 4,1643 (2013).

[5] A. Takeda, T. Aihara, M. Fukuhara, Y. Ishii, and M. Fukuda, "Schottky-type surface plasmon detector with nano-slit grating using enhanced resonant optical transmission", J. Appl. Phys. 116(8), 084313 (2014).

[6] B. Desiatov, I. Goykhman, N. Mazurski, J. Shappir, J. B. Khurgin, and U. Levy, "Plasmonic enhanced silicon pyramids for internal photoemission Schottky detectors in the near-infrared regime," Optica 2(4), 335–338 (2015).

[7] M. Alavirad, A. Olivieri, L. Roy, and P. Berini, "High-responsivity sub-bandgap hot-hole plasmonic Schottky detectors," Opt. Express 24(20), 22544–222554 (2016).

[8] M. Tanzid, A. Ahmadivand, R. Zhang, B. Cerjan, A. Sobhani, S. Yazdi, P. Nordlander, and N. J. Halas, "Combining Plasmonic Hot Carrier Generation with Free Carrier Absorption for High-Performance Near-Infrared Silicon-Based Photodetection," ACS Photonics 5(9), 3472–3477 (2018).

[9] A. Ono, K. Hashimoto, and N. Teranishi, "Near-infrared sensitivity improvement by plasmonic diffraction for a silicon image sensor with deep trench isolation filled with highly reflective metal," Opt. Express 29(14), 21313-21319 (2021).

[10] L. Gao, F. Lemarchand, and M. Lequime, "Refractive index determination of SiO2 layer in the UV/Vis/NIR range: spectrophotometric reverse engineering on single and bi-layer designs," J. Europ. Opt. Soc. Rap. Public. 8, 13010 (2013).

[11] K. M. McPeak, S. V. Jayanti, S. J. P. Kress, S. Meyer, S. Iotti, A. Rossinelli, and D. J. Norris, "Plasmonic films can easily be better: Rules and recipes," ACS Photonics 2(3), 326-333 (2015).

[12] A. D. Rakić, A. B. Djurišic, J. M. Elazar, and M. L. Majewski, "Optical properties of metallic films for vertical-cavity optoelectronic devices," Appl. Opt. 37(22), 5271-5283 (1998).